HOKKAIDO UNIVERSITY

Title	Valence-band-ordering of a strain-free bulk ZnO single crystal identified by four-wave-mixing spectroscopy technique
Author(s)	Hazu, K.; Chichibu, S. F.; Adachi, S. et al.
Citation	Journal of Applied Physics, 111(9), 093522 https://doi.org/10.1063/1.4711103
Issue Date	2012-05-01
Doc URL	https://hdl.handle.net/2115/49402
Rights	Copyright 2012 American Institute of Physics. This article may be downloaded for personal use only. Any other use requires prior permission of the author and the American Institute of Physics. The following article appeared in J. Appl. Phys. 111, 093522 (2012) and may be found at https://dx.doi.org/10.1063/1.4711103
Type	journal article
File Information	JAP111-9_093522.pdf

Hokkaido University Collection of Scholarly and Academic Papers : HUSCAP

AIP | Journal of Applied Physics

Valence-band-ordering of a strain-free bulk ZnO single crystal identified by four-wave-mixing spectroscopy technique

K. Hazu, S. F. Chichibu, S. Adachi, and T. Sota

Citation: J. Appl. Phys. **111**, 093522 (2012); doi: 10.1063/1.4711103
View online: http://dx.doi.org/10.1063/1.4711103
View Table of Contents: http://jap.aip.org/resource/1/JAPIAU/v111/i9
Published by the American Institute of Physics.

Related Articles

Depolarization effect on optical control of exciton states confined in GaAs thin films
J. Appl. Phys. 110, 043514 (2011)

Theoretical and experimental studies of surface plasmons excited at metal-uniaxial dielectric interface
Appl. Phys. Lett. 98, 021113 (2011)

Lateral spatial switching of excitons using vertical electric fields in semiconductor quantum rings
Appl. Phys. Lett. 97, 173101 (2010)

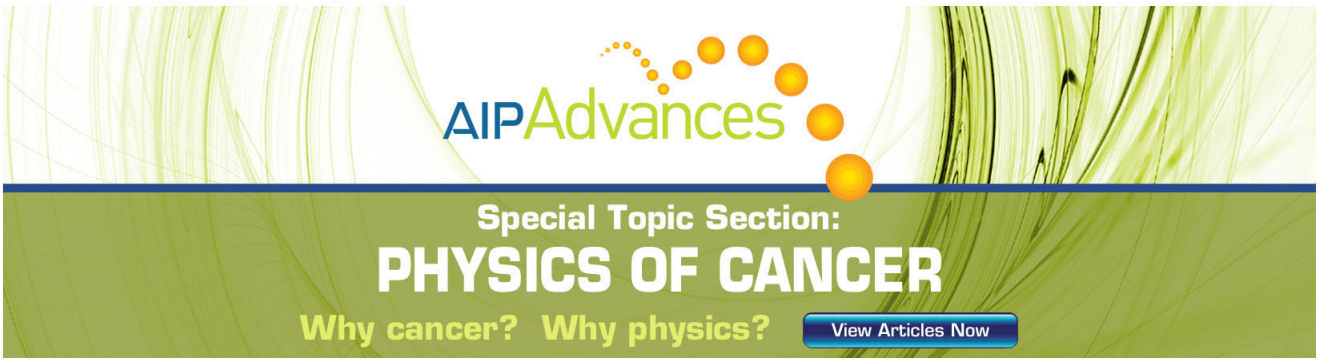
Enhanced exciton photoluminescence in the selectively Si-doped GaAs/AlxGa1−xAs heterostructures
J. Appl. Phys. 108, 063522 (2010)

Effect of correlation of local fluctuations on exciton coherence
J. Chem. Phys. 132, 204503 (2010)

Additional information on J. Appl. Phys.

Journal Homepage: http://jap.aip.org/
Journal Information: http://jap.aip.org/about/about_the_journal
Top downloads: http://jap.aip.org/features/most_downloaded
Information for Authors: http://jap.aip.org/authors

ADVERTISEMENT



Downloaded 18 Jun 2012 to 133.87.26.18. Redistribution subject to AIP license or copyright; see http://jap.aip.org/about/rights_and_permissions

Valence-band-ordering of a strain-free bulk ZnO single crystal identified by four-wave-mixing spectroscopy technique

K. Hazu,[1] S. F. Chichibu,[1,a)] S. Adachi,[2,b)] and T. Sota[3]
[1]*Institute of Multidisciplinary Research for Advanced Materials, Tohoku University, 2-1-1 Katahira, Aoba, Sendai 980-8577, Japan*
[2]*Department of Applied Physics, Hokkaido University, N13 W8, Kitaku, Sapporo 060-8628, Japan*
[3]*Department of Electrical Engineering and Bioscience, Waseda University, Tokyo 169-8555, Japan*

(Received 22 October 2011; accepted 9 April 2012; published online 7 May 2012)

Spectroscopic and temporal four-wave-mixing (FWM) measurements are carried out on a strain-free bulk ZnO single crystal, in order to clarify the valence-band-ordering. Under the collinearly polarized lights with the electric-field component parallel to the *c*-axis, which can excite dipole-allowed Γ_1-excitons, the FWM signal appears only in the energies corresponding to the B-exciton. Under the cross-linear polarization configuration exciting both Γ_5- and Γ_1-excitons, the FWM signal arising from the two-photon-coherence is absent in the energies corresponding to A-exciton. Both the results indicate that Γ_1-exciton state belongs exclusively to B-exciton, meaning that the valence-band ordering is $\Gamma_9 - \Gamma_7 - \Gamma_7$ in order of decreasing electron energy for the present strain-free ZnO single crystal. © *2012 American Institute of Physics*. [http://dx.doi.org/10.1063/1.4711103]

I. INTRODUCTION

Wurtzite (*wz*) zinc oxide (ZnO) and related group-II oxide semiconductors have attracted much attention as a promising candidate for potentially useful optoelectronic devices. As ZnO has a direct bandgap of 3.37 eV at room temperature[1] and the fundamental exciton binding energy is as high as 59 meV, applications to cost-competitive ultraviolet (UV) light-emitting diodes (LEDs)[2–5] have been expected. In addition, nonpolar-plane ZnO epitaxy has attracted increasing attention[6,7] as is the case with GaN and related alloys,[8] in order to design and fabricate light-polarization-sensitive optical devices. To quantitatively predict the optical anisotropy in ZnO, precise knowledge on the band structure and ordering is indispensable.

The symmetry ordering of valence bands (VBs) in *wz*-ZnO has long been subjected to extensive discussions since the first investigation on the exciton fine structure by Thomas in 1960.[1] The VBs of ZnO are known to arise from $2p^6$ states of oxygen atoms. The crystal field and spin-orbit interaction lift the degeneracy of the *p*-like states at the Γ point, leaving three separate VBs E_1, E_2, and E_3 in order of decreasing electron energy, as shown in Fig. 1(a). The transitions related to the respective VBs are labeled A-, B-, and C-transition. The excitons involved in the respective transitions are termed A-, B-, and C-excitons and abbreviated as X_A, X_B, and X_C. Numerous reports have emerged over the past 50 years postulating either Γ_9-symmetry[9–18] or Γ_7-symmetry[1,19–35] for the uppermost E_1 VB, as shown schematically on the right and left ends in Fig. 1(a), respectively. The energy splitting of the VBs due to the crystal-field (Δ_{cr}) and spin-orbit interaction (Δ_{so}) from zincblende (*zb*) symmetry to *wz* symmetry is shown merely schematically, representing the $\Gamma_7 - \Gamma_9 - \Gamma_7$ ordering on the left end and $\Gamma_9 - \Gamma_7 - \Gamma_7$ ordering on the right. The legends $\perp$ and $\parallel$ mean that the transitions are allowed for the light with the polarization configuration where the electric-field component (E) is perpendicular and is parallel to the optic *c*-axis ($E \perp c$ and $E \parallel c$), respectively. The parenthesis indicates that the transition is partially allowed, as listed in Table I.

Since the irreducible representation of the conduction band is Γ_7 for semiconductors belonging to point symmetry C_{6v}, for example, *wz*-ZnO and GaN, possible representations for A-exciton ground states are $\Gamma_1 \otimes \Gamma_7 \otimes \Gamma_7 = \Gamma_1 \oplus \Gamma_2 \oplus \Gamma_5$ in the case of Γ_7-symmetry, while $\Gamma_1 \otimes \Gamma_9 \otimes \Gamma_7 = \Gamma_5 \oplus \Gamma_6$ in the case of Γ_9-symmetry.[36] Here, Γ_1 on the left side of the equations is the representation for the envelope function of an exciton ground state. The excitons of Γ_5- and Γ_1-symmetry are dipole-allowed and called as *bright excitons*. Conversely, excitons of Γ_6- and Γ_2-symmetry are optically inactive and called as *dark excitons*. Therefore, the detection of Γ_1-excitons is a fingerprint that the transition involves a VB of Γ_7-state. The Γ_1-exciton is $E \parallel c$ polarized and Γ_5-exciton is $E \perp c$ polarized. However, the oscillator strength of Γ_1-exciton in B- (or A-) exciton manifold is far smaller than that of Γ_5-exciton. Therefore, it has been difficult to detect Γ_1-excitons apparently in most of previous studies, because linear spectroscopy techniques such as polarized reflectance, absorption, and photoluminescence (PL) measurements have been employed. For example, representative polarized reflectance spectra measured at 10 K for a quite low dislocation density, bowing-free, strain-free $(10\bar{1}0)$ *m*-plane bulk ZnO single crystal grown[37] by the hydrothermal method are displayed in Fig. 1(b). Although remarkable polarization dependence is found in the intensities for the ground-state ($n = 1$) and the first excited-state ($n = 2$) of exciton transitions, Γ_1-exciton feature cannot be apparently seen for either A- or B-exciton energy region of the spectrum taken under $E \parallel c$.

Alternative approaches for the VB-ordering identification have been proposed. One is to detect Γ_6-excitons despite its optical inactivity. For example, Γ_5- and Γ_6-excitons should exhibit different Zeeman splitting due to their different *g*-factors

a)Publishing author. Electronic mail: chichibulab@yahoo.co.jp.
b)Author to whom correspondence should be addressed. Electronic mail: adachi-s@eng.hokudai.ac.jp.

 © 2012 American Institute of Physics

Downloaded 18 Jun 2012 to 133.87.26.18. Redistribution subject to AIP license or copyright; see http://jap.aip.org/about/rights_and_permissions

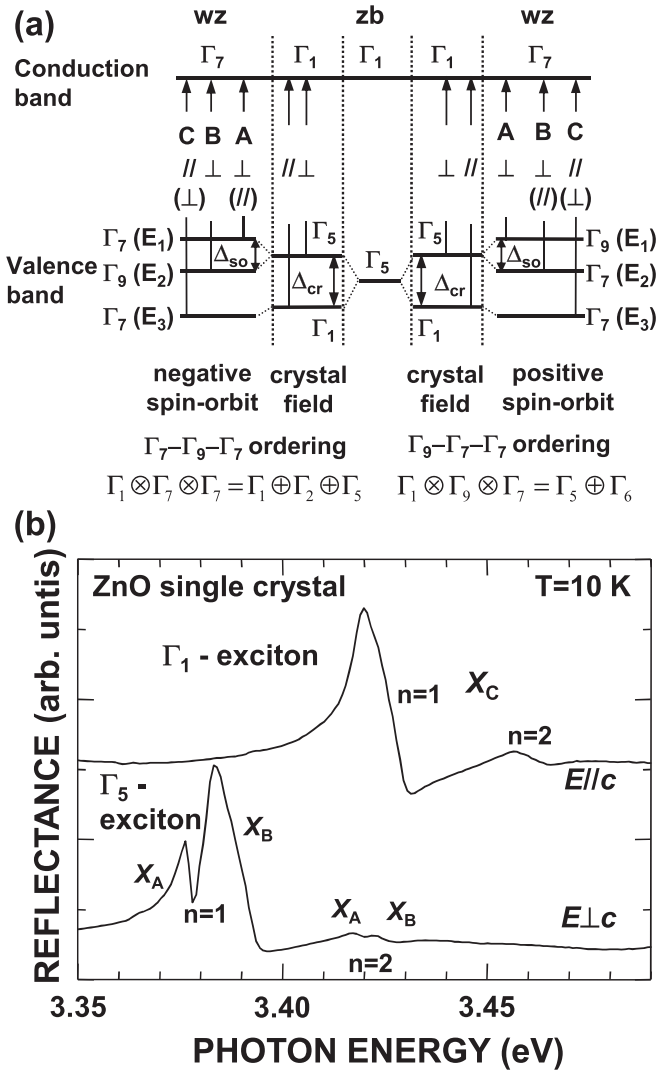


FIG. 1. (a) Band structure and labeling of A-, B-, and C-transitions expected in *wz*-ZnO. The crystal-field and spin-orbit interaction lift the degeneracy of the *p*-like Γ_5-states at the Γ point, leaving three separate E_1, E_2, and E_3 VBs in order of decreasing electron energy. The transitions related to the respective VBs are labeled A-, B-, and C-transition. The excitons involved in the respective transitions are termed A-, B-, and C-exciton and abbreviated as X_A, X_B, and X_C. Here, splitting of the VB due to the crystal-field (Δ_{cr}) and spin-orbit interaction (Δ_{so}) from *zb* symmetry to *wz* symmetry is shown merely schematically, representing the $\Gamma_7 - \Gamma_9 - \Gamma_7$ ordering on the left edge and $\Gamma_9 - \Gamma_7 - \Gamma_7$ ordering on the right. The legends $\perp$ and $\parallel$ mean that the transitions are allowed for the light with the polarization configuration electric-field component (E) perpendicular and parallel to the optic *c*-axis ($E \perp c$ and $E \parallel c$), respectively. The parenthesis indicates that the transition is partially allowed, as listed in Table I. Since the irreducible representation of the conduction band is Γ_7, possible representations for the A-exciton ground states are $\Gamma_1 \otimes \Gamma_7 \otimes \Gamma_7 = \Gamma_1 \oplus \Gamma_2 \oplus \Gamma_5$ in the case of Γ_7-symmetry, while $\Gamma_1 \otimes \Gamma_9 \otimes \Gamma_7 = \Gamma_5 \oplus \Gamma_6$ for Γ_9-symmetry.[36] The excitons of Γ_5- and Γ_1-symmetry are dipole-allowed and called as *bright excitons*. Conversely, excitons of Γ_6- and Γ_2-symmetry are optically inactive and called as *dark excitons*. (b) Representative polarized optical reflectance spectra measured at 10 K for a quite low dislocation density, bowing-free, strain-free $(10\bar{1}0)$ *m*-plane bulk ZnO single crystal grown[37] by the hydrothermal method.

$g_e^{\parallel} - g_h^{\parallel}$ and $g_e^{\parallel} + g_h^{\parallel}$, respectively. The values $g_e^{\parallel} \sim 1.95$ and $g_h^{\parallel} \sim 1.12$ have been reported for *c*-plane ZnO.[9] However, this discrimination is blurred and becomes marginal in magneto-photoluminescence (M-PL) measurement, because bound excitons that may have different momentum distribution from free-excitons are usually monitored and essentially weak

TABLE I. Relative intensities for the transitions involving the three separate valence bands in *wz*-ZnO.

	Relative intensities	
Valence band	$E \parallel C(\Gamma_1)$	$E \perp C(\Gamma_5)$
Γ_9	0	$\lvert P_2 \rvert^2$
Γ_7	$\frac{2E_3}{E_3-E_2}\lvert P_1 \rvert^2$	$\frac{E_2}{E_2-E_3}\lvert P_2 \rvert^2$
Γ_7	$\frac{2E_2}{E_2-E_3}\lvert P_1 \rvert^2$	$\frac{E_3}{E_3-E_2}\lvert P_2 \rvert^2$
	$E_1 = \Delta_1 + \Delta_2$	
	$E_{2,3} = \frac{\Delta_1-\Delta_2}{2} \pm \left[\left(\frac{\Delta_1-\Delta_2}{2}\right)^2 + 2\Delta_3^2\right]^{1/2}$	
	$P_1 = P_2$	
	$\Delta_1 = \Delta_{cr}$	
	$\Delta_2 = \Delta_3 = \frac{1}{3}\Delta_{so}$	

Γ_6-exciton peak is easily buried in the background signal, which consists of many PL lines for bound excitons of Γ_5-symmetry.

In order to avoid ambiguities and to experimentally settle the controversy, resonant excitation of optically active Γ_1- and Γ_5-excitons is a straightforward protocol, because the methodology stands on optical-transition selection rules. In more precise terms, collection of such signals from a background-free direction is preferable. The self-diffracted four-wave-mixing (FWM) technique aims at measuring the simplest coherent emission and has the following outstanding features: (i) resonant excitation is possible, (ii) FWM signals (I_{FWM}) are diffracted in the background-free direction, and (iii) I_{FWM} is proportional to the eighth power of the transition matrix elements (μ), i.e. $I_{FWM} \propto N^2\mu^8$, where N is exciton population. According to these features, FWM signals are quite sensitive to exciton polarization that can be investigated by changing the polarization direction of the incident excitation pulses. Therefore, degenerate FWM spectroscopy has been proved to be a powerful tool in providing much information on exciton dynamics and decay of coherence as well as on nonlinear mechanisms of exciton-photon interaction in the bulk and nanostructured semiconductors.[38] These intrinsic natures of FWM, for example, gave rise to clarification of the strain anisotropy in *wz*-GaN films grown on various substrates.[39–42]

In this article, the results of spectroscopic and temporal FWM measurements on a strain-free bulk ZnO single crystal are shown to identify Γ_1- and Γ_5-excitons. In Sec. II, details of the sample and experimental procedure of FWM are described. Because residual strain may modify the VB-ordering, we first verify that the sample is strain-free using the manner similar to Refs. 39–42 in Sec. III A. Then, energy-resolved and temporal FWM signals are obtained from a cleaved $\{10\bar{1}0\}$ surface ($k \perp c$) and a (0001) surface ($k \parallel c$) under various polarization combination of excitation pulses in Sec. III B. The collinearly and cross-linearly polarized FWM signals eventually give us the assignment that the exciton state with Γ_1-symmetry belongs to B-exciton. The results lead us to conclude consistently that VB-ordering is $\Gamma_9 - \Gamma_7 - \Gamma_7$ in order of decreasing electron energy in the present strain-free ZnO, which is similar to the *wz* families such as CdS (Ref. 36) and GaN (Refs. 43 and 44).

Downloaded 18 Jun 2012 to 133.87.26.18. Redistribution subject to AIP license or copyright; see http://jap.aip.org/about/rights_and_permissions

II. EXPERIMENTAL PROCEDURE

The ZnO sample measured in this study was a *c*-plane ZnO single crystal wafer grown by the seeded chemical vapor transport method.[9] The sample size was 10 mm × 10 mm × 500 μm, which enabled measuring various optical signals from a cleaved $\{10\bar{1}0\}$ *m*-plane. Polarized reflectance spectra similar to Fig. 1(b), photoreflectance spectra, and PL spectra for this particular sample have been given in Ref. 15.

The FWM measurements were carried out under the typical two-pulse self-diffraction geometry using a frequency-doubled mode-locked Al_2O_3:Ti laser with an 80 MHz repetition rate. The wavelength of the coherent pulses was tuned to A- and B-exciton resonances, namely approximately 360–370 nm. The laser bandwidth was 23 meV in those wavelengths (energies), which corresponds to the pulse width approximately 80 fs. The laser light was divided into two beams of equal intensities, and a sequence of two coherent pulses 1 and 2 with wave vectors k_1 and k_2, respectively, was spatially overlapped on the sample surface. The FWM process can be simply understood as follows. The first pulse (pulse 1), k_1, creates a coherent excitonic polarization. Then the second pulse (pulse 2) with a controlled delay time (τ_{12}) interferes the polarization and produces the polarization grating. The pulse 2 is thus self-diffracted by this grating into the direction $2k_2 - k_1$, which is a completely background-free direction. Accordingly, the decay of the grating can also be monitored by the second pulse, until the coherence of excitonic polarization produced by the first pulse completely relaxes. Therefore, the signal represents the phase relaxation of the excitonic polarization. The value of τ_{12} was controlled by a stepping motor-driven optical delay line, where τ_{12} takes positive value when the pulse 1 (k_1) precedes the pulse 2 (k_2). The signal at each τ_{12} was dispersed by a 0.35-m-focal-length grating monochromator equipped with a 2400 grooves/mm grating and was detected by a CCD detector. The spectral resolution was 0.45 meV at a wavelength of around 370 nm. Throughout the FWM measurements, the sample temperature was kept at 10 K. Most of the data were taken from cleaved $\{10\bar{1}0\}$ surface ($k\perp c$). The signals were also measured for (0001) surface ($k \parallel c$) for comparison.

III. RESULTS AND DISCUSSION

A. Strain anisotropy analysis

It is well known that VB-mixing changes the corresponding exciton eigen-states and induces the exchange in their oscillator strengths. Anisotropic residual strain may induce a VB-mixing and may change the polarization of excitons, as intensively studied for (Al,In,Ga)N films and quantum wells fabricated on nonpolar and semipolar planes.[8] The degree of anisotropy may vary from nearly zero (pure biaxial strain) to uniaxial strain as the upper limit. If the stain mixes the topmost E_1 and E_2 VBs of ZnO, the polarization of Γ_5-exciton changes from the cross-circular eigenstates ($|\uparrow\rangle$ and $|\downarrow\rangle$, or σ_+ and σ_-) to the cross-linear eigenstates ($|\uparrow\rangle \pm |\downarrow\rangle$, or x and y), where $\uparrow$ and $\downarrow$ indicate the exciton spin direction. Combining with the anisotropic exchange interaction, those new eigenstates split energetically and show an exciton fine structure.[45] This phenomenon has been found in GaN epilayers grown on foreign substrates suffering from in-plane uniaxial compressive stress[39–42] and also in self-assembled GaN quantum dots, which suffer from anisotropic stresses.[46,47]

In order to verify if the present ZnO sample is strain-free (even locally), the strain anisotropy analysis is carried out with the aid of the high sensitivity of FWM to exciton polarizations: the FWM response is proportional to the fourth power of the transition oscillator strength $|\mu|^2$. Indeed, this advantage plays an important role in detecting strain anisotropy even for the epilayers grown on isotropic substrates and bulk samples, in which only negligible strain anisotropy is expected.[42] The experimental configuration and the results are shown in Fig. 2. As shown in Fig. 2(a), the excitation pulses with the same intensities (<0.3 mW/pulse) were collinearly polarized, and focused beams were superimposed onto the sample surface through a lens ($k \parallel c$). The focused spot diameter was approximately ~100 μm. In this geometry, Γ_5-excitons are exclusively excited. The in-plane linear-polarization angle (θ) can be rotated using a half-wave-plate (HWP) mounted on a rotating stage. The excitation energy was tuned so that the excitation laser bandwidth covered the energies of A- and B-excitons, as shown by the dashed curve in Fig. 2(b). The energies corresponding to A- and B-excitons, which have been obtained through the theoretical fitting of the polarized reflectance spectrum for ($k \parallel c, E\perp c$) at 10 K (Ref. 15), are indicated by the angle brackets labeled X_A and X_B, respectively. As shown, A- and B-excitons were simultaneously excited, and the FWM spectrum for $\tau_{12} = 0.01$ ps and $\theta = 0°$ was obtained. By rotating the excitation collinear polarization, the degree of linear polarization of excitons, which reflects the in-plane strain anisotropy, can be examined with very high sensitivity. Figure 2(c) shows the ratio of FWM signal intensities for A- and B-excitons, which is defined as $(I^A_{FWM} - I^B_{FWM})/(I^A_{FWM} + I^B_{FWM})$, as a function of the polarization angle θ. Here, I^A_{FWM} and I^B_{FWM} are the FWM signal intensities for A- and B-excitons, respectively. If the sample has certain in-plane strain anisotropy, for example GaN epilayers grown on an *a*-plane Al_2O_3 substrate,[39,42] the FWM intensity ratio exhibits a sinusoidal curve varying from almost −1 to 1 due to the exchange in oscillator strengths arising from $E_1 - E_2$ VB-mixing. However, the value is almost constant for the present ZnO sample: the amplitude is 0.026 by a sinusoidal fitting. In addition, exciton fine structure splitting is not observed for the energies corresponding to A- and B-exciton manifold within our spectral resolution. The results indicate that the present sample is free from in-plane strain anisotropy.[48]

B. FWM signals from the cleaved $\{10\bar{1}0\}$ plane

Among the *bright excitons*, because Γ_1-exciton is produced only from the transition between Γ_7 conduction band and Γ_7 VB,[49] the VB-ordering can be definitely determined from the energy at which Γ_1-exciton structure appears. Therefore, the detection and energy determination of Γ_1- and Γ_5-excitons are the most important purpose of this study. As Γ_1-exciton is $E \parallel c$ polarized, it can be excited with linearly $E \parallel c$ polarized light on a cleaved $\{10\bar{1}0\}$ plane. On the other hand, Γ_5-exciton is $E\perp c$ polarized and it can be excited

Downloaded 18 Jun 2012 to 133.87.26.18. Redistribution subject to AIP license or copyright; see http://jap.aip.org/about/rights_and_permissions

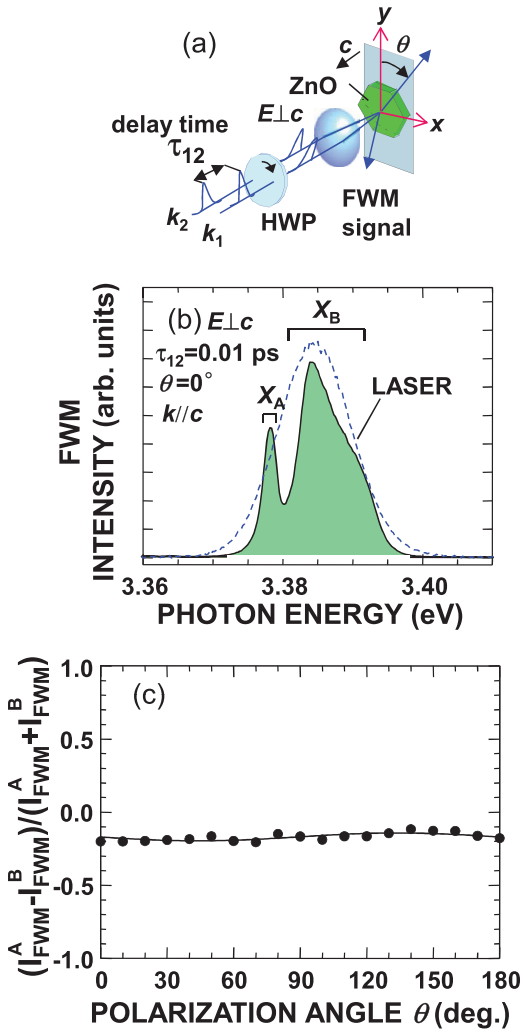


FIG. 2. (a) Experimental setup for the in-plane strain anisotropy measurements by a two-pulse FWM configuration. The polarization configuration for the collinear light is ($k \parallel c, E \perp c$). The excitation laser light was divided into two beams of equal intensities, and a sequence of two coherent pulses 1 and 2 with wave vectors k_1 and k_2, respectively, was spatially overlapped on the sample surface. The wavelength of the coherent pulses was tuned to A- and B-exciton resonances. The excitons coherently created by the first pulse interfere and produce an excitonic polarization grating. The second pulse (pulse 2) with a controlled delay time (τ_{12}) was diffracted by this grating into the direction $2k_2 - k_1$, which is a background-free direction. (b) Representative spectrally resolved FWM signal at $\tau_{12} = 0.01$ ps and $\theta = 0°$. The excitation laser spectrum is also shown by dashed curve (blue online). Two angle brackets labeled X_A and X_B indicate the energies corresponding to Γ_5 A- and B-excitons, respectively. (c) The ratio of the FWM signal intensities for A- and B-excitons, which is defined as $(I^A_{FWM} - I^B_{FWM})/(I^A_{FWM} + I^B_{FWM})$, as a function of the polarization angle θ. I^A_{FWM} and I^B_{FWM} are the FWM signal intensities for A- and B-excitons, respectively, and θ is the half angle of the HWP rotation.

effectively on both $\{10\bar{1}0\}$ and (0001) planes. Therefore, Γ_1- and Γ_5-excitons can be distinguished from polarized FWM signals taken from a plane containing the c-axis parallel to the surface, such as m-plane in this case, as shown in Fig. 3(a).

Energy-resolved FWM signals measured under the collinear polarization for $\tau_{12} = 0.01$ ps are shown in Fig. 3(b). The solid (black online) and dotted (red online) curves are the signals measured under $E \perp c$ and $E \parallel c$ polarizations, respectively. The laser spectrum is also shown by the dashed (blue online) curve. The angle brackets labeled X_A and X_B show the energies for A- and B-excitons, respectively.

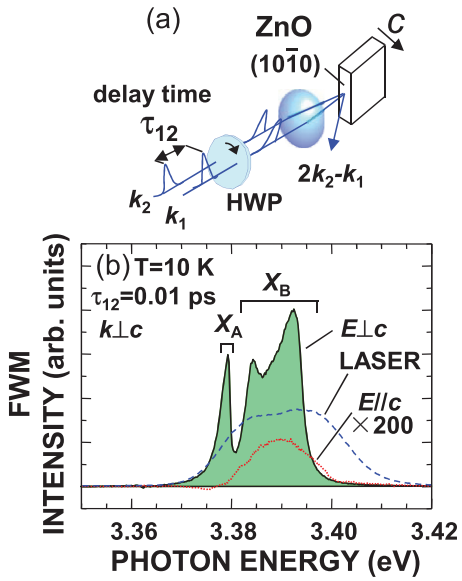


FIG. 3. (a) Experimental setup for the two-pulse FWM measurement using collinearly polarized lights ($k \perp c$). The wavelength of the coherent pulses was tuned to A- and B-exciton resonances. (b) Energy-resolved FWM spectra for the strain-free ZnO bulk single crystal taken under the light polarization $E \perp c$ (solid curve) and $E \parallel c$ (dotted curve, red). Two angle brackets labeled X_A and X_B indicate the energies corresponding to Γ_5 A- and B-excitons, respectively. The excitation laser spectrum is also shown by the dashed curve (blue).

As shown, a sharp peak at the energy corresponding to A-exciton and a double-peaked broad band at the energy covering B-exciton manifold are observed for $E \perp c$ polarization. The value of full-width at half-maximum (FWHM) for the A-exciton peak is approximately 1.6 meV, which is smaller than the longitudinal-transverse splitting (ω_{LT}) for the Γ_5 A-exciton ($\omega_{LT,A}$) being 2.0 meV for this particular sample.[15] The band at around B-exciton is revealed by the spectral deconvolution procedure to contain three components. Similar to the A-exciton peak, FWHM value for each deconvoluted component is smaller than ω_{LT} for the Γ_5 B-exciton ($\omega_{LT,B}$) being 10.9 meV (Ref. 15).

The FWM signal intensity for $E \perp c$ in Fig. 3(b) is more than two orders of magnitude larger than the $E \parallel c$ case, and the signals are detected in the energies covering both A- and B-excitons. The result is consistent with the fact that $E \perp c$ polarized Γ_5-exciton is involved in both A- and B-excitons. On the other hand, weak FWM signal is detected only within the energies for B-excitons under $E \parallel c$ polarization. The result clearly indicates that Γ_1-exciton state belongs to B-exciton, meaning that the valence-band ordering should be $E_1 - \Gamma_9, E_2 - \Gamma_7$, and $E_3 - \Gamma_7$, as shown on the right end in Fig. 1(a).

It should be noted that the interaction between Γ_5- and Γ_1-excitons is one of the characteristics for the transition represented by $\Gamma_1 \otimes \Gamma_7 \otimes \Gamma_7$: FWM signals have been observed under all polarization configurations for the C-exciton manifold,[50] which involves Γ_5- and Γ_1-excitons. Paradoxically, if the topmost E_1 VB belongs to the irreducible representation Γ_7, A-exciton should have both Γ_1- and Γ_5-states. Then, FWM signal originating from A-excitons is supposed to appear under both collinear and cross-linear

Downloaded 18 Jun 2012 to 133.87.26.18. Redistribution subject to AIP license or copyright; see http://jap.aip.org/about/rights_and_permissions

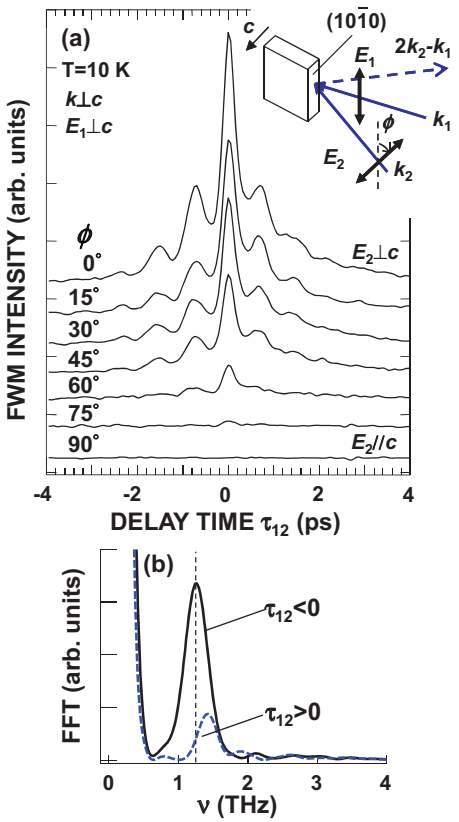


FIG. 4. (a) Temporal FWM signals monitored at the photon energy corresponding mainly to A-exciton in the strain-free ZnO single crystal measured under $k_1 \perp c$ and $k_2 \perp c$ as a function of ϕ, where ϕ denotes the angle between the polarization vectors for k_1 and k_2 pulses. The former (E_1) is set perpendicular to the c-axis, while the angle ϕ was varied from $\phi = 0°$ ($E_1 \perp c, E_2 \perp c$) to $\phi = 90°$ ($E_1 \perp c, E_2 \parallel c$). The inset shows the experimental configuration. For $\phi = 0°$, Γ_5-states of both A- and B-excitons are excited, while Γ_1-excitons can be excited especially for $\phi = 90°$ (b) Fast-Fourier-transformed signals of the collinearly polarized ($E_1 \perp c, E_2 \perp c : \phi = 0°$) FWM signals for $\tau_{12} < 0$ and $\tau_{12} > 0$.

excitation configurations. For example, FWM signal should be observed for the cross-linear configuration ($E_1 \perp c$, $E_2 \parallel c$), which corresponds to the polarization rotation angle (ϕ) of E_2 relative to E_1 in the inset of Fig. 4(a) is 90°. Here, E_1 is set perpendicular to the c-axis ($E_1 \perp c$). This should be remarkable for the negative delay times ($\tau_{12} < 0$), where the two-photon-coherence (TPC) according to the two-photon absorption by E_2 would dominate the FWM signal in the $2k_2 - k_1$ direction.[51] To examine this, FWM signals were measured as a function of τ_{12}. The FWM intensities measured using the excitation laser with the central photon energy of 3.372 eV, which mainly covers the energy of A-exciton, are shown as functions of τ_{12} and ϕ in Fig. 4(a). For $\phi = 0°$ ($E_1 \perp c, E_2 \perp c$), a remarkable beating structure is found for $\tau_{12} < 0$. The beating period is 0.79 ps (5.23 meV), which agrees with the beating period originating from the quantum interference between $XX_{AA} - X_A^T$ and $XX_{AB} - X_A^T$ transitions,[52] where XX_{AA}, XX_{AB}, X_A^T, and X_B^T are AA-homo-biexciton, AB-hetero-biexciton, transverse A-exciton, and transverse B-exciton, respectively. For $\tau_{12} > 0$, the beating period is 0.70 ps (5.91 meV), indicating that the beating may originate from the $X_A^T - X_B^T$ quantum interference.[52] Significant difference between the beating periods for $\tau_{12} < 0$ and $\tau_{12} > 0$ can be seen in the fast-Fourier-transformed (FFT) signals drawn in Fig. 4(b). With respect to the ϕ dependence, the amplitude of the FWM signal decreases with the increase in ϕ and completely vanishes for the cross-linear excitation, $\phi = 90°$ ($E_1 \perp c, E_2 \parallel c$). As stated above, the signal induced by TPC should appear even for $\phi = 90°$ if A-exciton belongs to Γ_7-symmetry (A-exciton contains Γ_1-state). Therefore, Γ_1 state is not involved in A-exciton. Finally, we emphasize again that FWM signal is extremely sensitive to the oscillator strength of the transition ($\propto \mu^8$), and Γ_1-excitons excited by $E \parallel c$ polarized light never respond within the energies covering the A-exciton in our strain-free ZnO sample.

IV. CONCLUSION

Spectroscopic and temporal, self-diffracted degenerate FWM measurements were carried out on the strain-free bulk ZnO single crystal, in order to clarify the VB-ordering. Under $E \parallel c$ polarization that can excite dipole-allowed Γ_1-excitons exclusively, the collinearly polarized FWM signal appears only within the energies corresponding to the B-exciton. Within the energies mainly cover the A-exciton, FWM signals originating from two-photon coherence were absent for both $\tau_{12} < 0$ and $\tau_{12} > 0$ under the cross-linear excitation configuration, where Γ_5- and Γ_1-excitons can be simultaneously excited with a desired time delay. Both the results indicate that Γ_1-exciton state belongs to B-exciton, meaning that the valence-band-ordering is $\Gamma_9 - \Gamma_7 - \Gamma_7$ in order of decreasing electron energy in the present strain-free ZnO single crystal.

ACKNOWLEDGMENTS

The authors would like to thank Dr. G. Cantwell and Dr. D. C. Reynolds for providing the high-quality bulk ZnO single crystal. This work was supported in part by Grant-in Aids of Scientific Research No. 22246037 under MEXT, Japan and AOARD/AFOSR. S.F.C. would like to offer tributes to departed saint Cole Litton.

[1]D. G. Thomas, J. Phys. Chem. Solids **15**, 86 (1960).
[2]A. Tsukazaki, A. Ohtomo, T. Onuma, M. Ohtani, T. Makino, M. Sumiya, K. Ohtani, S. F. Chichibu, S. Fuke, Y. Segawa, H. Ohno, H. Koinuma, and M. Kawasaki, Nature Mater. **4**, 42 (2005).
[3]A. Tsukazaki, M. Kubota, A. Ohtomo, T. Onuma, K. Ohtani, H. Ohno, S. F. Chichibu, and M. Kawasaki, Jpn. J. Appl. Phys. **44**, L643 (2005).
[4]Ü. Özgür, Y. I. Alivov, C. Liu, A. Teke, M. A. Reshchikov, S. Dogan, V. Avrutin, S. J. Cho, and H. Morkoç, J. Appl. Phys. **98**, 041301 (2005).
[5]C. Klingshirn, Phys. Status Solidi B **244**, 3027 (2007).
[6]M. Wraback, H. Shen, S. Liang, C. R. Gorla, and Y. Lu, Appl. Phys. Lett. **74**, 507 (1999).
[7]T. Koida, S. F. Chichibu, A. Uedono, T. Sota, A. Tsukazaki, and M. Kawasaki, Appl. Phys. Lett. **84**, 1079 (2004).
[8]Review article for nonpolar and semipolar group-III nitride semiconductors, see for example, the special issue of MRS Bull introduced by J. S. Speck and S. F. Chichibu, MRS Bull. **34**, 304 (2009).
[9]D. C. Reynolds, C. W. Litton, and T. C. Collins, Phys. Rev. **140**, A1726 (1965).
[10]Y. S. Park, C. W. Litton, T. C. Collins, and D. C. Reynolds, Phys. Rev. **143**, 512 (1966).
[11]D. C. Reynolds and T. C. Collins, Phys. Rev. **185**, 1099 (1969).
[12]D. C. Reynolds, D. C. Look, B. Jogai, C. W. Litton, G. Cantwell, and W. C. Harsch, Phys. Rev. B **60**, 2340 (1999).

Downloaded 18 Jun 2012 to 133.87.26.18. Redistribution subject to AIP license or copyright; see http://jap.aip.org/about/rights_and_permissions

[13]D. C. Reynolds, D. C. Look, B. Jogai, C. W. Litton, T. C. Collins, M. T. Harris, M. J. Callahan, and J. S. Bailey, J. Appl. Phys. **86**, 5598 (1999).
[14]B. Gil, Phys. Rev. B **64**, 201310(R) (2001).
[15]S. F. Chichibu, T. Sota, G. Cantwell, D. B. Eason, and C. W. Litton, J. Appl. Phys. **93**, 756 (2003).
[16]S. F. Chichibu, A. Uedono, A. Tsukazaki, T. Onuma, M. Zamfirescu, A. Ohtomo, A. Kavokin, G. Cantwell, C. W. Litton, T. Sota, and M. Kawasaki, Semicond. Sci. Technol. **20**, S67 (2005).
[17]S. Adachi, K. Hazu, T. Sota, S. Chichibu, G. Cantwell, D. C. Reynolds, and C. W. Litton, Phys. Status Solidi C **2**, 890 (2005).
[18]S. Adachi, J. Lumin. **12**, 34 (2005).
[19]W. Y. Liang and A. D. Yoffe, Phys. Rev. Lett. **20**, 59 (1968).
[20]W. R. L. Lambrecht, A. V. Rodina, S. Limpijumnong, B. Segall, and B. K. Meyer, Phys. Rev. B **65**, 075207 (2002).
[21]A. V. Rodina, M. Strassburg, M. Dworzak, U. Haboeck, A. Hoffmann, A. Zeuner, H. R. Alves, D. M. Hofmann, and B. K. Meyer, Phys. Rev. B **69**, 125206 (2004).
[22]J. J. Hopfield, J. Phys. Chem. Solids **15**, 97 (1960).
[23]B. Segall, Phys. Rev. **163**, 769 (1967).
[24]K. Hümmer, Phys. Status Solidi B **86**, 527 (1978).
[25]P. Loose, M. Rosenzweig, and M. Wohlecke, Phys. Status Solidi B **75**, 137 (1976).
[26]K. Hümmer, R. Helbig, and M. Baumgärtner, Phys. Status Solidi B **56**, 249 (1973).
[27]G. Blattner, C. Klingshirn, R. Helbig, and R. Meinl, Phys. Status Solidi B **107**, 105 (1981).
[28]G. Blattner, G. Kurtze, G. Schmieder, and C. Klingshirn, Phys. Rev. B **25**, 7413 (1982).
[29]J. Gutowski, N. Presser, and I. Broser, Phys. Rev. B **38**, 9746 (1988).
[30]M. Fiebig, D. Frohlich, and C. Pahlke-Lerch, Phys. Status Solidi B **177**, 187 (1993).
[31]J. Wrzesinski and D. Fröhlich, Solid State Commun. **105**, 301 (1998).
[32]R. Laskowski and N. E. Christensen, Phys. Rev. B **73**, 045201 (2006).
[33]M. Goano, F. Bertazzi, M. Penna, and E. Bellotti, J. Appl. Phys. **102**, 083709 (2007).
[34]L. Ding, B. K. Li, H. T. He, W. K. Ge, J. N. Wang, J. Q. Ning, X. M. Dai, C. C. Ling, and S. J. Xu, J. Appl. Phys. **105**, 053511 (2009).
[35]M. R. Wagner, J-H. Schulze, R. Kirste, M. Cobet, A. Hoffmann, C. Rauch, A. V. Rodina, B. K. Meyer, U. RNoder, and K. Thonke, Phys. Rev. B **80**, 205203 (2009).
[36]B. Hönerlage, R. Lévy, J. B. Grun, C. Klingshirn, and K. Bohnert, Phys. Rep. **124**, 161 (1985) and references cited therein.
[37]K. Maeda, M. Sato, I. Niikura, and T. Fukuda, Semicond. Sci. Technol. **20**, S49 (2005).
[38]J. Shah, *Ultrafast Spectroscopy of Semiconductors and Semiconductor Nanostructures* (Springer-Verlag, New York, 1998).
[39]Y. Toda, S. Adachi, Y. Abe, K. Hoshino, and Y. Arakawa, Phys. Rev. B **71**, 195315 (2005).
[40]Y. Toda, T. Ishiguro, S. Adachi, K. Hoshino, and Y. Arakawa, Phys. Status Solidi B **245**, 878 (2008).
[41]T. Ishiguro, Y. Toda, S. Adachi, T. Mukai, K. Hoshino, and Y. Arakawa, Phys. Status Solidi B **243**, 1560 (2006).
[42]S. Adachi, Y. Toda, T. Ishiguro, K. Hoshino, and Y. Arakawa, Phys. Status Solidi C **3**, 1595 (2006).
[43]R. Dingle, D. D. Sell, S. E. Stokowski, and M. Ilegems, Phys. Rev. B **4**, 1211 (1971).
[44]For example, see A. Shikanai, T. Azuhata, T. Sota, S. Chichibu, A. Kuramata, K. Horino, and S. Nakamura, J. Appl. Phys. **81**, 417 (1997).
[45]M. Bayer, G. Ortner, O. Stern, A. Kuther, A. A. Gorbunov, A. Forchel, P. Hawrylak, S. Fafard, K. Hinzer, T. L. Reinecke, S. N. Walck, J. P. Reithmaier, F. Klopf, and F. Schafer, Phys. Rev. B **65**, 195315 (2002).
[46]Y. Léger, L. Besombes, L. Maingault, and H. Mariette, Phys. Rev. B **76**, 045331 (2007).
[47]S. Ohno, S. Adachi, R. Kaji, S. Muto, and H. Sasakura, Appl. Phys. Lett. **98**, 161912 (2011).
[48]At present, we have not yet confirmed whether the strain anisotropy does not exist over the whole region of the sample. However, its demonstration is beyond the scope of this work.
[49]G. L. Bir and G. E. Pickus, *Symmetry and Strain-Induced Effects in Semiconductors* (Wiley, New York, 1974).
[50]K. Hazu, K. Torii, T. Sota, S. Adachi, SF. Chichibu, G. Cantwell, D. C. Reynolds, and C. W. Litton, J. Appl. Phys. **95**, 5498 (2004).
[51]K. B. Ferrio and D. G. Steel, Phys. Rev. B **54**, R5231 (1996).
[52]K. Hazu, T. Sota, K. Suzuki, S. Adachi, SF. Chichibu, G. Cantwell, D. B. Eason, D. C. Reynolds, and C. W. Litton, Phys. Rev. B **68**, 033205 (2003).

Downloaded 18 Jun 2012 to 133.87.26.18. Redistribution subject to AIP license or copyright; see http://jap.aip.org/about/rights_and_permissions